

Discussion

The synthetic chemistry presented here offers straightforward, general routes to a broad family of ether- and halide-free bis-(pentamethylcyclopentadienyl)lanthanide alkyls and hydrides. The hydrides are of course greatly desirable synthetic targets for catalytic studies but are equally valuable precursors for numerous types of ether- and halide-free lanthanide hydrocarbyls and other derivatives.⁴ One result of this work is thus a readily accessible, homologous series of tractable, thermally stable, very electrophilic (for which there is structural evidence), and very highly reactive lanthanide alkyl/hydride pairs which span the 4f block from the lightest (4f⁰) to the heaviest member (4f¹⁴). In chemistry involving olefins, significant reactivity differences are observed between light (La, Nd) and heavy (Lu) lanthanides. For example, the light members appear to be the most active "homogeneous" ethylene polymerization catalysts prepared to date. For bulkier olefins, allylic C-H activation and η^3 -allyl formation are found to compete

with olefin insertion into the metal-carbon σ bond. This fine structure is by no means predicted and will be explored further in our following discussions of $\text{Me}_2\text{SiCp}''_2$ lanthanide chemistry¹³ and organolanthanide-catalyzed olefin hydrogenation chemistry.¹⁵

Acknowledgment. This research was supported by a grant from MolyCorp. We thank Dr. Mark Delaney of Dow Chemical Co. Central Research Laboratories for GPC data and helpful advice. G. J. and H. L. thank the Fonds der Chemischen Industrie for fellowship support during their stay in the United States.

Registry No. 1, 98720-34-4; 2, 78128-14-0; 3, 98720-35-5; 4, 78128-06-0; 5, 98720-36-6; 6, 93383-00-7; 7, 98720-37-7; 8, 98720-38-8; 10, 98720-39-9; 10d, 98720-41-3; 11, 93303-98-1; 11d, 98720-42-4; 12, 84751-30-4; 12d, 98720-43-5; 13, 98720-40-2; 13d, 98720-48-0; 14, 98720-49-1; 15, 98720-52-6; 16, 98720-50-4; 17, 98735-43-4; 18, 98720-44-6; 19, 98720-45-7; 20, 98720-46-8; 21, 98720-47-9; LaCl_3 , 10099-58-8; LiCp' , 51905-34-1; $(\text{Cp}'_2\text{LaCl}_2)_2$, 98735-44-5; $\text{LiCH}(\text{TMS})_2$, 41823-71-6; SmCl_3 , 10361-82-7; C_6D_6 , 1076-43-3; propylene, 115-07-1; ethylene, 74-85-1; polyethylene, 9002-88-4; 1-hexene, 592-41-6; butadiene, 106-99-0; cyclohexene, 110-83-8; 5-deuterio-7-(deuteriomethyl)-undecane, 98720-51-5; 1-hexene/ethylene copolymer, 25213-02-9.

Supplementary Material Available: Table of anisotropic thermal parameters for non-hydrogen atoms (Table III) and listing of observed and calculated structure factors from the final cycle of least-squares refinement and ¹³C NMR spectra of the 1-hexene dimer $\text{C}_{12}\text{H}_{24}\text{D}_2$ (51 pages). Ordering information given on any current masthead page.

Highly Reactive Organolanthanides. Synthesis, Chemistry, and Structures of 4f Hydrocarbyls and Hydrides with Chelating Bis(polymethylcyclopentadienyl) Ligands

Gerald Jeske,^{1a} Laurel E. Schock,^{1b} Paul N. Swepston,^{1c} Herbert Schumann,^{1d} and Tobin J. Marks*^{1e}

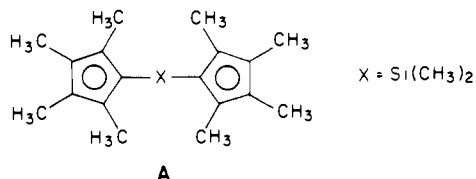
Contribution from the Department of Chemistry, Northwestern University, Evanston, Illinois 60201, and the Institut für Anorganische und Analytische Chemie, Technische Universität Berlin, D-1000 Berlin 12, Bundesrepublik Deutschland. Received April 29, 1985

Abstract: This contribution discusses lanthanide hydrocarbyl and hydride chemistry based upon $\text{Me}_2\text{SiCp}''_2$ supporting ligation ($\text{Cp}'' = \eta^5\text{-(CH}_3)_4\text{C}_5$). The reaction of MCl_3 , $\text{M} = \text{Nd, Sm, or Lu}$, with $\text{Me}_2\text{Si}(\text{Cp}''\text{Li})_2$ yields the precursor complexes $\text{Me}_2\text{SiCp}''_2\text{MCl}_2\text{-Li}(\text{ether})_2^+$. A slightly different workup procedure yielded $(\text{Me}_2\text{SiCp}''_2\text{NdCl})_2\text{Cl-Li}(\text{THF})_2^+$, which crystallizes in the monoclinic space group $P2_1/n$ with two molecules in a unit cell of dimensions (-133°C) $a = 11.666$ (3) Å, $b = 12.585$ (3) Å, $c = 17.765$ (6) Å, and $\beta = 94.91$ (2)°. Least-squares refinement led to a value for the conventional R index (on F) of 0.045 for 3231 independent reflections having $I > 3\sigma(I)$. The structure consists of two $\text{Me}_2\text{Si}(\eta^5\text{-Cp}''_2)_2\text{Nd}$ units bridged by a chloride ion and an $\text{Nd-Cl}\cdots\text{Li}^+\cdots\text{Cl}^-\cdots\text{Nd}$ linkage. The Nd-Cl distances are 2.802 (1) and 2.754 (2) Å, and $\angle\text{Cl-Nd-Cl} = 97.1$ (1)°. The (ring centroid)-Nd-(ring centroid) angle is 121.3°. The Nd-C(ring) distances vary from 2.647 (7) to 2.815 (7) Å, with the shorter distances being to those carbon atoms closest to the Me_2Si bridge. The $\text{Me}_2\text{SiCp}''_2\text{MCl}_2$ compounds react with $\text{LiCH}[\text{Si}(\text{CH}_3)_2]_2$ to yield ether- and halide-free $\text{Me}_2\text{SiCp}''_2\text{MCH}[\text{Si}(\text{CH}_3)_2]_2$ derivatives. The $\text{M} = \text{Nd}$ compound crystallizes in the monoclinic space group $P2_1/n$ with four molecules in a cell of dimensions (-125°C) $a = 10.229$ (2) Å, $b = 15.623$ (3) Å, $c = 19.687$ (3) Å, and $\beta = 105.41$ (2)°. Least-squares refinement led to a value of the conventional R index (on F) of 0.044 for 3407 independent, absorption corrected reflections having $I > 3\sigma(I)$. The molecular structure consists of monomeric $\text{Me}_2\text{SiCp}''_2\text{NdCH}[\text{Si}(\text{CH}_3)_2]_2$ units with $\eta^5\text{-Cp}''$ coordination, and $\angle(\text{ring centroid})\text{-Nd-(ring centroid)} = 121.6^\circ$. The $\text{CH}[\text{Si}(\text{CH}_3)_2]_2$ fragment is coordinated to the $\text{Me}_2\text{SiCp}''_2\text{Nd}$ center in a highly unsymmetrical fashion with a Nd-C σ -bond distance of 2.506 (7) Å and a secondary interaction to one methyl group of $\text{Nd-C} = 2.862$ (8) Å. The Si-C distance to this carbon atom is significantly longer than the other Si-CH₃ contacts. Approximate hydrogen atom locations argue against an important $\text{M}\cdots\text{HC}$ (methyl) interaction and reveal a bending of the hydrogen atom on the σ -bonded carbon atom toward the metal with $\angle\text{Nd-C-H} \sim 76^\circ$. Reaction of the $\text{Me}_2\text{SiCp}''_2\text{MCH}[\text{Si}(\text{CH}_3)_2]_2$ complexes with H_2 yields the corresponding hydrides, which are formulated as $\text{Me}_2\text{SiCp}''_2\text{M}(\mu\text{-H})_2\text{MCp}''_2\text{SiMe}_2$ dimers. These compounds are active agents for the polymerization of ethylene as well as for the oligomerization of propylene and 1-hexene. For a constant lanthanide ion, a $(\text{Me}_2\text{SiCp}''_2\text{MH})_2$ hydride is an ca. 10 times more active for this reaction than the corresponding $(\text{Cp}'_2\text{MH})_2$ hydride. Deprotonation of $\text{Me}_2\text{SiCp}''_2\text{LuCH}(\text{TMS})_2$ with $t\text{-BuLi/TMEDA}$ leads to a metallacycle formulated as $\text{Li}(\text{TMEDA})_3^+\text{-Me}_2\text{SiCp}''_2\text{LuCH}_2\text{Si}(\text{CH}_3)_2\text{C}(\text{H})\text{Si}(\text{CH}_3)_3^-$.

In the previous paper in this issue,² we describe general, straightforward synthetic approaches to and chemical/physico-

chemical properties of the 4f hydrocarbyls and hydrides $\text{Cp}'_2\text{MR}$ ($\text{Cp}' = \eta^5\text{-(CH}_3)_5\text{C}_5$, $\text{R} = \text{CH}[\text{Si}(\text{CH}_3)_2]_2$) and $(\text{Cp}'_2\text{MH})_2$, where

M = the lightest to heaviest lanthanide. The molecular structure of $\text{Cp}'_2\text{NdCH}(\text{TMS})_2$ ($\text{TMS} = \text{Si}(\text{CH}_3)_3$) features an unusual "semibridging" $\text{Nd}\cdots\text{CH}_3$ interaction. The hydrides are some of the most active "homogeneous" ethylene polymerization and olefin hydrogenation catalysts yet discovered.^{2,3} To the extent that these characteristics reflect factors such as coordinative unsaturation and the disposition/mobility of the Cp' ligands, it would be of interest to further "open" the lanthanide coordination sphere. We describe here the synthesis, structural characterization, and some chemical properties of a new class of lanthanide hydrocarbyls and hydrides based upon the chelating bis(polymethylcyclopentadienyl) ligand **A** ($\text{Me}_2\text{SiCp}'_2$).^{4,5} Straightforward, general routes to



$\text{CH}(\text{TMS})_2$ and hydride derivatives are reported for lanthanides from Nd to Lu. We have previously described a series of organo-actinide complexes of this ligand and reported substantial (up to 10^3) enhancements in catalytic activity over $\text{Cp}'_2\text{Th}$ analogues.⁶ For the present case of lanthanides, ligand **A** also offers the possibility of reducing solid-state Cp' structural disorder and undesirable $\text{Cp}'_2\text{M} \rightarrow \text{Cp}'\text{M}$ ligand redistribution processes.⁷

Experimental Section

Procedures, synthetic techniques, materials, and instrumentation were as described previously.² The ligand $\text{Me}_2\text{Si}(\text{Cp}'\text{Li})_2$ and the dilithium salt $\text{Me}_2\text{Si}(\text{Cp}'\text{Li})_2$ were prepared as described elsewhere.^{4,6} Mass spectra of solids were recorded at 70 eV by using the direct injection technique.

$\text{Me}_2\text{SiCp}'_2\text{NdCl}_2\text{-Li}(\text{ether})_2^+$ (1). A suspension of 0.500 g (2.00 mmol) of NdCl_3 and 0.623 g (2.00 mmol) of $\text{Me}_2\text{Si}(\text{Cp}'\text{Li})_2$ in 60 mL of THF was refluxed for 12 h. The THF was removed in vacuo and the residue extracted with 50 mL of diethyl ether. The ether extract was filtered and cooled to -30°C to yield, after decantation of the solvent and vacuum drying, 0.84 g (63%) of $\text{Me}_2\text{SiCp}'_2\text{NdCl}_2\text{-Li}(\text{ether})_2^+$ as pale-green crystals: IR data (Nujol mull, cm^{-1}) 2720 (w), 1347 (w), 1317 (s), 1250 (s), 1240 (s), 1190 (m), 1150 (m), 1125 (m), 1092 (s), 1055 (s), 1010 (s), 940 (w), 910 (m), 900 (m), 832 (s), 808 (s), 780 (m), 757 (s), 665 (s); ^1H NMR (toluene- d_8 , 0°C) δ 26.66 (s, br, 12 H), 2.86 (s, br, 8 H), 0.66 (s, br, 12 H), -1.98 (s, br, 6 H), -12.96 (s, br, 12 H). Anal. Calcd for $\text{C}_{28}\text{H}_{50}\text{SiCl}_2\text{LiO}_2\text{Nd}$: C, 50.28; H, 7.54; Si, 4.20; Li, 1.04; Nd, 21.56. Found: C, 50.37; H, 7.49; Si, 4.25; Li, 1.06; Nd, 21.70.

$\text{Me}_2\text{SiCp}'_2\text{LuCl}_2\text{-Li}(\text{ether})_2^+$ (3). The above procedure was carried out with 0.500 g (1.78 mmol) of LuCl_3 , 0.560 g (1.79 mmol) of $\text{Me}_2\text{Si}(\text{Cp}'\text{Li})_2$, and 50 mL of THF. Workup as before yielded 0.60 g (48%) of $\text{Me}_2\text{SiCp}'_2\text{LuCl}_2\text{-Li}(\text{ether})_2^+$ as colorless crystals: IR data (KBr, cm^{-1}) 2905 (vs), 2720 (w), 1445 (s), 1385 (s), 1345 (w), 1310 (s), 1250 (s), 1240 (s), 1215 (vs), 1185 (m), 1152 (m), 1125 (m), 1095 (s), 1060 (s), 1020 (s), 950 (w), 910 (m), 890 (m), 830 (s), 810 (s), 780 (m), 758 (s), 700 (s), 555 (vw), 500 (w), 460 (s), 375 (w), 300 (w); ^1H NMR (toluene- d_8) δ 3.27 (q, 8 H), 2.22 (s, 12 H), 2.12 (s, 12 H), 1.04 (s, 6 H + t, 12 H). Anal. Calcd for $\text{C}_{28}\text{H}_{50}\text{SiCl}_2\text{LiO}_2\text{Lu}$: C, 48.07; H, 7.20;

Si, 4.01. Found: C, 48.05; H, 7.15; Si, 4.05.

$\text{Me}_2\text{SiCp}'_2\text{NdCH}(\text{TMS})_2$ (5). A mixture of 1.09 g (1.63 mmol) of $\text{Me}_2\text{SiCp}'_2\text{NdCl}_2\text{-Li}(\text{ether})_2^+$ and 0.270 g (1.62 mmol) of $\text{LiCH}(\text{TMS})_2$ was suspended in 50 mL of toluene at -78°C . The suspension was gradually allowed to warm to room temperature overnight with stirring. Next, the toluene was removed in vacuo, and the green residue was extracted with 50 mL of pentane, filtered, and cooled to 0°C . Subsequent decantation of the supernatant and vacuum drying yielded 0.94 g (95%) of $\text{Me}_2\text{SiCp}'_2\text{NdCH}(\text{TMS})_2$ as a green, microcrystalline solid: IR (KBr, cm^{-1}) 2900 (vs), 1440 (m), 1375 (m), 1342 (w), 1310 (m), 1242 (s), 1120 (m), 1042 (s), 1008 (m), 940 (vw), 860 (s), 820 (s), 755 (m), 690 (w), 670 (m), 560 (m), 450 (m), 368 (m), 295 (m); ^1H NMR (toluene- d_8) δ 136.0 (s, br, 1 H), 15.4 (s, br, 6 H), 10.7 (s, br, 6 H), 8.0 (s, br, 6 H), -9.2 (s, br, 6 H), -14.1 (s, br, 18 H), -17.4 (s, br, 6 H). Anal. Calcd for $\text{C}_{27}\text{H}_{49}\text{Si}_3\text{Nd}$: C, 53.86; H, 8.20; Si, 13.99; Nd, 23.95. Found: C, 53.80; H, 8.14; Si, 13.86; Nd, 24.10.

$\text{Me}_2\text{SiCp}'_2\text{SmCH}(\text{TMS})_2$ (6). **One-Pot Synthesis.** A mixture of 0.500 g (1.95 mmol) of SmCl_3 and 0.61 g (1.95 mmol) of $\text{Me}_2\text{Si}(\text{Cp}'\text{Li})_2$ was refluxed in 50 mL of THF for 12 h. Next, the solvent was removed under high vacuum, and 0.32 g (1.92 mmol) of $\text{LiCH}(\text{TMS})_2$ was added to the solid residue. The mixture was then suspended in toluene at -78°C and gradually allowed to warm to room temperature with stirring. Evaporation of the toluene and recrystallization from pentane yielded 0.77 g (65%) of $\text{Me}_2\text{SiCp}'_2\text{SmCH}(\text{TMS})_2$ as an orange, microcrystalline solid: IR (KBr, cm^{-1}) 2900 (s), 1440 (m), 1385 (m), 1350 (w), 1315 (m), 1250 (s), 1120 (m), 1050 (s), 1020 (m), 950 (w), 860 (s), 830 (s), 760 (m), 675 (m), 575 (m), 454 (m), 380 (m), 300 (m); ^1H NMR (toluene- d_8) δ 20.59 (s, 1 H), 2.52 (s, 6 H), 2.50 (s, 6 H), 2.39 (s, 6 H), -4.01 (s, 6 H), -4.30 (s, 6 H), -5.48 (s, 18 H). Anal. Calcd for $\text{C}_{27}\text{H}_{49}\text{Si}_3\text{Sm}$: C, 53.31; H, 8.12; Si, 13.85; Sm, 24.72. Found: C, 54.69; H, 8.29; Si, 13.38; Sm, 23.72.

$\text{Me}_2\text{SiCp}'_2\text{LuCH}(\text{TMS})_2$ (7). The procedure described above for $\text{Me}_2\text{SiCp}'_2\text{NdCH}(\text{TMS})_2$ was followed with 0.60 g (0.86 mmol) of $\text{Me}_2\text{SiCp}'_2\text{LuCl}_2\text{-Li}(\text{ether})_2^+$ and 0.14 g (0.84 mmol) of $\text{LiCH}(\text{TMS})_2$ in 50 mL of toluene: yield 0.49 g (90%) of $\text{Me}_2\text{SiCp}'_2\text{LuCH}(\text{TMS})_2$ as colorless crystals; IR (KBr, cm^{-1}) 2900 (vs), 1560 (vw), 1440 (m), 1375 (m), 1345 (w), 1312 (m), 1242 (s), 1120 (m), 1040 (s), 1010 (m), 860 (s), 815 (s), 755 (m), 690 (w), 665 (m), 575 (m), 455 (m), 375 (m), 295 (m); ^1H NMR (Toluene- d_8) δ 1.958 (s, 6 H), 1.946 (s, 6 H), 1.934 (s, 6 H), 1.851 (s, 6 H), 0.917 (s, 6 H), 0.061 (s, 18 H), -0.411 (s, 1 H). Anal. Calcd for $\text{C}_{27}\text{H}_{49}\text{Si}_3\text{Lu}$: C, 51.24; H, 7.80. Found: C, 51.35; H, 7.84.

$(\text{Me}_2\text{SiCp}'_2\text{NdH})_2$ (13). A solution of 0.940 g (1.56 mmol) of $\text{Me}_2\text{SiCp}'_2\text{NdCH}(\text{TMS})_2$ in 50 mL of pentane was stirred for 12 h under 1 atm of H_2 (the reaction appears visually to be complete in less than 1 h). After this time, the resulting precipitate was isolated by filtration, washed with several portions of pentane, and vacuum-dried to yield 0.68 g (98%) $(\text{Me}_2\text{SiCp}'_2\text{NdH})_2$ as a green, microcrystalline solid. The deuterated analogue was prepared in a similar manner when using D_2 : IR (KBr, cm^{-1}) 2900 (s), 1435 (m), 1380 (m), 1325 (s), 1251 (s), 1198 (s), 1122 (s, br), 1050 (m), 1015 (m), 950 (vw), 835 (s), 811 (s), 790 (vw), 760 (m), 670 (s), 565 (m), 438 (m), 382 (m), 295 (w); for $(\text{Me}_2\text{SiCp}'_2\text{NdD})_2$ 2900 (s), 1400 (w), 1345 (s), 1320 (s), 1315 (s), 1252 (s), 1145 (s), 1010 (m), 850 (vw), 830 (s, br), 760 (m), 665 (s); ^1H NMR (toluene- d_8) δ 26.40 (s, 6 H), -5.421 (s, 12 H), -9.562 (s, 12 H), the hydride signal could not be located. Anal. Calcd for $\text{C}_{20}\text{H}_{31}\text{Si}_2\text{Nd}$: C, 54.13; H, 7.04; Si, 6.33; Nd, 32.50; M_r 888. Found: C, 53.89; H, 7.09; Si, 6.52; Nd, 32.38; M_r 765 \pm 10% (cryoscopic in benzene).

$(\text{Me}_2\text{SiCp}'_2\text{SmH})_2$ (14). The above procedure was carried out with 0.370 g (0.610 mmol) of $\text{Me}_2\text{SiCp}'_2\text{SmCH}(\text{TMS})_2$ in 40 mL of pentane: yield 0.250 g (91%) of $(\text{Me}_2\text{SiCp}'_2\text{SmH})_2$ as an orange, microcrystalline solid: IR (KBr, cm^{-1}) 1440 (m), 1380 (m), 1334 (s), 1250 (m, br), 1125 (m), 1015 (m), 950 (vw), 835 (s), 810 (s), 758 (m), 669 (s), 590 (m, br), 450 (m), 380 (m), 300 (m); ^1H NMR (toluene- d_8 , under H_2) δ 5.34 (s, br, < 1 H), 2.58 (s, 6 H), -0.38 (s, 12 H), -2.65 (s, 12 H); mass spectrum m/e 949 (dimer), 932 (dimer - ICH_4), 473 (monomer). Anal. Calcd for $\text{C}_{20}\text{H}_{31}\text{Si}_2\text{Sm}$: C, 53.39; H, 6.95; Si, 6.24; Sm, 33.42. Found: C, 53.43; H, 6.86; Si, 6.19; Sm, 33.50.

$(\text{Me}_2\text{SiCp}'_2\text{LuH})_2$ (15). Following the above procedure for $(\text{Me}_2\text{SiCp}'_2\text{NdH})_2$, 0.490 g (0.779 mmol) of $\text{Me}_2\text{SiCp}'_2\text{LuCH}(\text{TMS})_2$ was hydrogenolyzed in 50 mL of pentane: yield 0.330 g (90%) of $(\text{Me}_2\text{SiCp}'_2\text{LuH})_2$ as a colorless microcrystalline solid. The deuterio derivative was synthesized in a similar manner when using D_2 : IR (KBr, cm^{-1}) 2900 (s), 1428 (m), 1380 (m), 1322 (m), 1245 (s), 1220 (m, br), 1126 (m), 1035 (m, br), 1011 (m), 910 (m), 832 (s), 810 (s), 760 (m), 660 (s), 440 (m), 430 (m), 420 (m), 380 (w), 300 (w); for $(\text{Me}_2\text{SiCp}'_2\text{LuD})_2$ 2900 (s), 1440 (m, br), 1388 (m), 1330 (m, br), 1255 (s), 1132 (m), 1040 (m, br), 965 (m, br), 836 (s), 814 (s), 760 (m), 670 (s), 560 (m), 450 (w), 420 (w), 380 (w), 300 (w); ^1H NMR (toluene- d_8 , under H_2) δ 9.252 (s, 1 H), 2.105 (s, 12 H), 2.026 (s, 12 H), 0.955 (s,

(1) (a) Technische Universität Berlin. Work performed while a visiting scholar at Northwestern University. (b) Northwestern University. Diffraction study of $(\text{Me}_2\text{SiCp}'_2\text{NdCl}_2\text{Cl-Li}(\text{THF})_2^+)$. (c) Staff crystallographer, Northwestern University. (d) Technische Universität Berlin. (e) Northwestern University.

(2) Jeske, G.; Lauke, H.; Mauermann, H.; Swepston, P. N.; Schumann, H.; Marks, T. J. *J. Am. Chem. Soc.*, previous paper in this issue.

(3) Jeske, G.; Lauke, H.; Mauermann, H.; Schumann, H.; Marks, T. J. *J. Am. Chem. Soc.*, following paper in this issue.

(4) Mintz, E. A.; Schertz, L. D.; Marks, T. J., manuscript in preparation.

(5) For the use of chelating C_5H_4 ligands in organo-f-element chemistry, see: (a) Secaur, C. A.; Day, V. W.; Ernst, R. D.; Kennelly, W. J.; Marks, T. J. *J. Am. Chem. Soc.* **1976**, *98*, 3713-3715. (b) Marks, T. J. *Adv. Chem. Ser.* **1976**, *150*, 232-255. (c) Qian, C.; Ye, C.; Lu, H.; Li, Y.; Huang, Y. *J. Organomet. Chem.* **1984**, *263*, 333-343 and references therein. (d) John, J. N.; Tsutsui, M. *Inorg. Chem.* **1981**, *20*, 1602-1604.

(6) (a) Fendrick, C. M.; Mintz, E. A.; Schertz, L. D.; Marks, T. J.; Day, V. W. *Organometallics* **1984**, *3*, 819-821. (b) Fendrick, C. M.; Day, V. W.; Marks, T. J., submitted for publication.

(7) Watson, P. L.; Whitney, J. F.; Harlow, R. L. *Inorg. Chem.* **1981**, *20*, 3271-3278.

Table I. Crystallographic Details

complex	(Me ₂ SiCp'' ₂ NdCl) ₂ Cl ⁻ Li ⁺ (THF) ₂ ⁺ (4)	Me ₂ SiCp'' ₂ NdCH(TMS) ₂ (5)
space group	P2 ₁ /n	P2 ₁ /n
a, Å	11.666 (3)	10.229 (2)
b, Å	12.585 (3)	15.623 (3)
c, Å	17.765 (6)	19.687 (3)
β, deg	94.91 (2)	105.41 (2)
volume, Å ³	2597.3	3031.9
Z	2	4
density (calcd), g cm ⁻³	1.538	1.319
cryst dimensions	0.1 × 0.05 × (0.1–0.3) mm (irregular)	
radiation	Mo Kα graphite monochromator	Mo Kα graphite monochromator
linear absorption coeff, cm ⁻¹	44.4	18.47
temp, K	140	148
scan mode	ω/2θ	ω/2θ
2θ limit	50.0°	50.0°
scan range	1.2°	1.2°
data collected	±h, +k, +l	±h, +k, +l
unique data	4722	5317
unique data with I > 3σ(I)	3231	3407
final no. of variables	263	281
R(F)	0.045	0.044
R _w (F)	0.061	0.058
GOF	1.497	1.534

6 H). Anal. Calcd for C₂₀H₃₁SiLu: C, 50.62; H, 6.59. Found: C, 50.43; H, 6.21.

Deprotonation of Me₂SiCp''₂LuCH(TMS)₂. A -78 °C solution of 0.360 g (0.569 mmol) of Me₂SiCp''₂LuCH(TMS)₂ and 0.30 mL of tetramethylethylenediamine (TMEDA) in 50 mL of pentane was slowly treated with 0.30 mL (0.60 mmol) of *tert*-butyllithium (2 N in hexane). A colorless solid began to precipitate immediately, and a gas was evolved. The reaction mixture was next warmed to room temperature, and the precipitate was collected by filtration, washed with several portions of pentane, and dried under high vacuum: yield 0.50 g (89%) of Me₂SiCp''₂LuCH[Si(CH₃)₂CH₂]TMS⁻Li⁺(TMEDA)₃ (11) as a colorless, microcrystalline solid; IR (KBr, cm⁻¹) 2900 (vs), 1465 (s), 1410 (w), 1380 (w), 1360 (m), 1340 (w), 1312 (s), 1290 (s), 1245 (s), 1230 (s), 1180 (m), 1160 (m), 1127 (s), 1098 (m), 1076 (m), 1045 (s), 1030 (s), 1010 (s), 945 (s), 810 (vs), 750 (s), 690 (s), 665 (s), 600 (m), 585 (w), 565 (m), 460 (s), 430 (m), 380 (m), 335 (m), 280 (w); ¹H NMR (THF-d₈) δ 2.30 (s, 12 H, TMEDA), 2.15 (s, 36 H, TMEDA), 2.12 (s, 6 H), 1.98 (s, 3 H), 1.93 (s, 6 H), 1.88 (s, 3 H), 1.82 (s, 6 H), 0.72 (s, 3 H), 0.66 (s, 3 H), -0.13 (s, 6 H), -0.17 (s, 9 H), -0.98 (d, 1 H, J = 14 Hz), -0.93 (d, 1 H, J = 14 Hz), -1.72 (s, 1 H). Anal. Calcd for C₄₅H₉₆N₆Si₃LiLu: C, 54.74; H, 9.80; N, 8.51; Lu, 17.72. Found: C, 54.54; H, 9.89; N, 8.55; Lu, 17.92.

Olefin Polymerization and Oligomerization Experiments. The apparatus and methodology were the same as that for the analogous (Cp''₂MH)₂ studies.²

X-ray Crystallographic Study of (Me₂SiCp''₂NdCl)₂Cl⁻Li⁺(THF)₂⁺ (4).⁸ Irregular, light-blue crystals suitable for diffraction studies were obtained by extracting the crude solid reaction product of NdCl₃ + Me₂Si(Cp''Li)₂ in THF with pentane, filtering, and slowly cooling the filtrate. The crystals were sealed in glass capillaries and examined on an Enraf-Nonius CAD4 automated diffractometer at 140 K. Monoclinic symmetry was inferred from the unit cell parameters and confirmed by analysis of symmetry equivalent intensities. Systematic extinctions were consistent with the space group P2₁/n. Accurate unit cell parameters were determined by least-squares refinement of 25 high-angle reflections. Three-dimensional data were collected (4722 unique reflections having 2θ_{MoKα} < 50°) by using graphite monochromated Mo radiation and ω/2θ scans (ω scan width = 1.2° + 0.35 tan θ°). Crystal and/or instrumental instability was monitored through the measurement of six standard reflections that were collected after every 100 min of X-ray exposure time; there was no indication of crystal decomposition. Experimental details are given in Table I.

All calculations were performed on a VAX 11/730 computer with the SDP crystallographic software package⁹ and programs standard in this

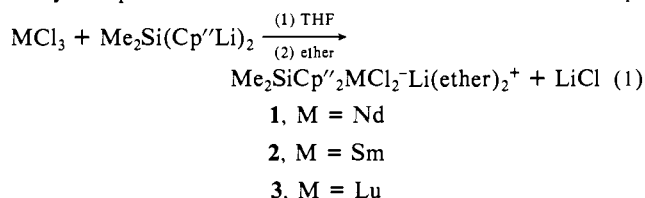
laboratory. Due to the irregular shape of the crystal, numerical absorption corrections were not performed. Since psi scans indicated that absorption was not a serious problem, empirical corrections¹⁰ were also not applied. Neutral atom scattering factors¹¹ were used with anomalous dispersion corrections¹² being applied to the non-hydrogen atoms.¹³ The structure was solved by standard Patterson and Fourier methods. Structural parameters were refined anisotropically to convergence, and the final agreement indexes are given in Table I. Hydrogen atoms were located from difference Fourier calculations but were not included in the model. The maximum peak height in the final difference electron density map was 1.140 e/Å³.

X-ray Crystallographic Study of Me₂SiCp''₂NdCH(TMS)₂ (5).⁸ Green crystals of Me₂SiCp''₂NdCH(TMS)₂ suitable for diffraction studies were obtained by slow cooling of saturated pentane solutions to -30 °C. The crystals were sealed in glass capillaries and examined on the aforementioned diffractometer at 148 K. They were found to be monoclinic, space group P2₁/n. Accurate unit cell parameters (Table I) were determined by least-squares refinement of 21 high-angle reflections. Three-dimensional data were collected (5317 unique reflections having 2θ_{MoKα} < 50°) by using graphite monochromated Mo radiation and ω/2θ scans (ω scan width = 1.2° + 0.35 tan θ°). Crystal and/or instrumental instability was monitored through the measurement of six standard reflections that were collected after every 100 min of X-ray exposure time; there was no indication of crystal decomposition. Experimental details are compiled in Table I.

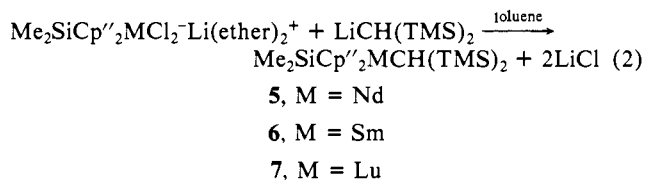
Calculations were performed by using the hardware and software described above. The intensity data were corrected for absorption effects by using an empirical absorption curve based upon psi scan data.¹⁰ The structure was solved by standard Patterson and Fourier methods. Neutral atom scattering factors¹¹ were used with anomalous dispersion corrections¹² being applied to the non-hydrogen atoms.¹³ Structural parameters were refined to convergence as described in Table I. Hydrogen atoms were located in the difference Fourier calculation but were not specifically included in the refinement model. The maximum peak height in the final difference Fourier synthesis was 0.89 e/Å³.

Results and Discussion

Synthesis. Halo Precursors and Hydrocarbyls. For lanthanides Nd, Sm, and Lu, tractable halo complexes of the Me₂SiCp''₂ ligand are readily accessible via the approach of eq 1. These complexes were characterized by standard spectroscopic and analytical procedures. In a situation reminiscent of, but ap-



parently more severe than, the Cp''₂M complexes,² difficulty was encountered in the lanthanum synthesis. Intractable products were obtained under all workup conditions. For the NdCl₃ reaction, a different workup procedure, using pentane rather than ether for extraction of the crude reaction product, yielded a crystalline material which was shown by X-ray diffraction to be (Me₂SiCp''₂NdCl)₂Cl⁻Li⁺(THF)₂⁺ (4, *vide infra*). Complexes 1–3 are readily converted to the CH(TMS)₂ derivatives (eq 2).



Judging from results with Sm (see Experimental Section), it should also be possible to synthesize 5 and 7 by a "one-pot" procedure

(9) Enraf-Nonius Structure Determination Package.

(10) North, A. T.; Phillips, D. C.; Mathews, F. S. *Acta Crystallogr., Sect. A* 1968, **A24**, 351.

(11) Cromer, D. T.; Waber, J. T. "International Tables for X-ray Crystallography"; The Kynoch Press: Birmingham, England, 1974; Vol. IV, Table 2.2B.

(12) Ibers, J. A.; Hamilton, W. C. *Acta Crystallogr.* 1964, **17**, 781–782.

(13) Cromer, D. T. "International Tables for X-ray Crystallography"; The Kynoch Press: Birmingham, England, 1974; Vol. IV, Table 2.3.1.

(8) See paragraph at end of paper regarding supplementary material.

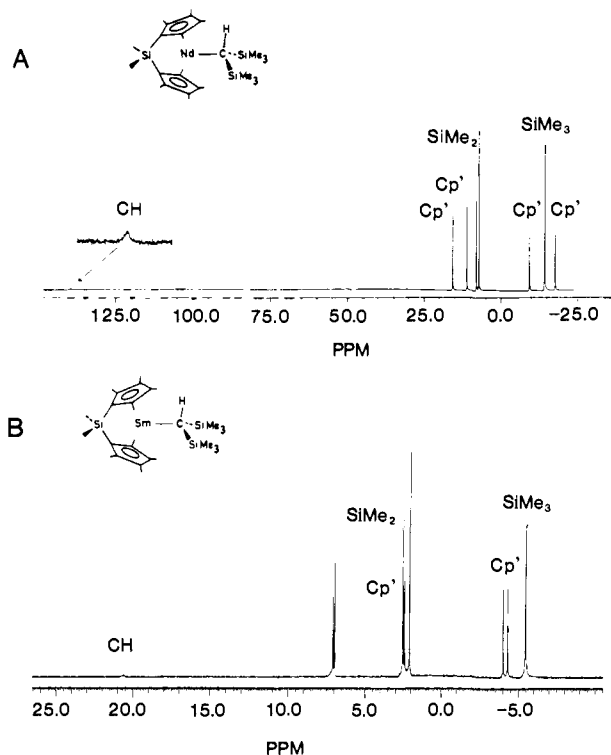


Figure 1. ^1H NMR spectra (90 MHz) of the paramagnetic organolanthanides: (A) $\text{Me}_2\text{SiCp}'_2\text{NdCH}(\text{TMS})_2$ (**5**) in benzene- d_6 (the resonance at δ 7.15 is due to benzene- d_6) and (B) $\text{Me}_2\text{SiCp}'_2\text{SmCH}(\text{TMS})_2$ (**6**) in toluene- d_8 (the resonances at δ 2.08 and 7.00 are due to toluene- d_7).

(and possibly a lanthanum hydrocarbyl). Complexes **5–7** are crystalline, pentane-soluble materials that appear to be indefinitely stable at room temperature. As for the $\text{Cp}'_2\text{MCH}(\text{TMS})_2$ derivatives,² the ^1H NMR spectra of **5–7** reveal magnetically equivalent $\text{Si}(\text{CH}_3)_3$ units (with magnetically equivalent CH_3 groups within each unit) and magnetically nonequivalent $(\text{CH}_3)_4\text{C}_5$

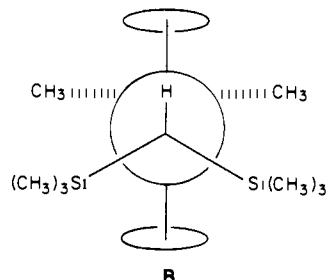


Figure 2. Perspective ORTEP drawing of the non-hydrogen atoms of $(\text{Me}_2\text{SiCp}'_2\text{NdCl})_2\text{Cl}^-\text{Li}^+(\text{THF})_2^+$ (**4**). All atoms are represented by thermal vibrational ellipsoids drawn to encompass 50% of the electron density.

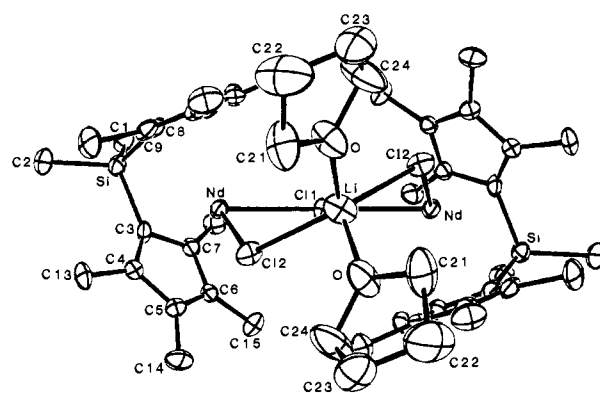


Figure 3. Perspective ORTEP view of the non-hydrogen atoms of $(\text{Me}_2\text{SiCp}'_2\text{NdCl})_2\text{Cl}^-\text{Li}^+(\text{THF})_2^+$ (**4**) along the Li^+ to bridging Cl^- vector. All atoms are represented by ellipsoids drawn to encompass 50% of the electron density.

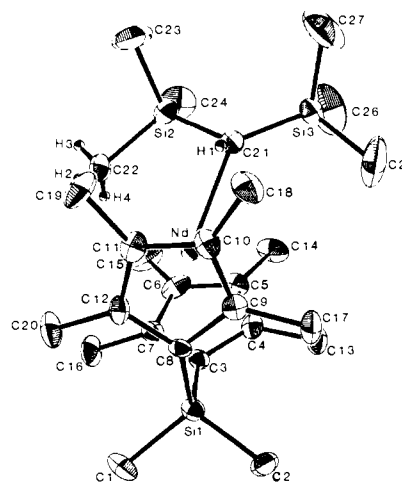


Figure 4. Perspective ORTEP drawing of the molecular structure of $\text{Me}_2\text{SiCp}'_2\text{NdCH}(\text{TMS})_2$ (**5**). Only selected hydrogen atoms are shown. All non-hydrogen atoms are represented by thermal vibrational ellipsoids drawn to encompass 50% of the electron density.

and that for $(\text{CH}_3)_4\text{C}_5$ ring interconversion is large. rings, suggestive of conformation **B**. The paramagnetic Nd and Sm derivatives exhibit large isotropic shifts. Some representative spectra are shown in Figure 1. Except for monotonic, temperature-dependent variations in isotropic shifts, which are typical of paramagnetic f-element complexes, ^1H NMR spectra of **5** were independent of temperature between -90 and $+90$ $^\circ\text{C}$. Thus, the free-energy barrier to $\text{Si}-\text{CH}_3$ group interconversion is small and that for $(\text{CH}_3)_4\text{C}_5$ ring interconversion is large.

Molecular Structure of $(\text{Me}_2\text{SiCp}'_2\text{NdCl})_2\text{Cl}^-\text{Li}^+(\text{THF})_2^+$ (4**).** As can be seen in Figures 3 and 4, the molecular structure of **4** is in effect a dimer, consisting of two $\text{Me}_2\text{SiCp}'_2\text{Nd}$ units bridged by a $\text{Cl}^-\text{Li}^+\text{Cl}^-$ assembly (reminiscent of $[\text{CH}_2(\text{C}_5\text{H}_4)_2\text{UCl}_2]_2\text{Cl}^-\text{Li}^+(\text{THF})_2^{5a}$). The molecule possesses a crystallographic 2-fold axis extending through the lithium ion and the single bridging chloride (C11). Final atomic coordinates and anisotropic thermal parameters are given in Tables II and III,⁸ respectively, while important bond lengths and angles are given along with estimated standard deviations in Table IV (the atom labeling scheme is shown in Figures 2 and 3).

The coordination pattern about the Nd^{3+} ion(s) in **4** is a modification of the common $\text{Cp}'_2\text{MX}_2$ type.^{2,7,14,15} It differs in

that, as a consequence of the Me_2Si bridge, the (ring centroid)–M–(ring centroid) angle has contracted from the usual $135\text{--}140^\circ$ to 121.3° . An analogous effect is observed on pro-

(14) Watson, P. L.; Parshall, G. W. *Acc. Chem. Res.* **1985**, *18*, 51–56.
 (15) (a) Tilley, T. D.; Andersen, R. A. *Inorg. Chem.* **1981**, *20*, 3267–3270.
 (b) Tilley, T. D.; Andersen, R. A.; Zalkin, A. *Inorg. Chem.* **1983**, *22*, 856–859.
 (c) Tilley, T. D.; Andersen, R. A. *J. Am. Chem. Soc.* **1982**, *104*, 1772–1774.

Table II. Positional Parameters and Their Estimated Standard Deviations for $(\text{Me}_2\text{SiCp}'_2\text{NdCl}_2)_2\text{Cl-Li}(\text{THF})_2^+$ (**4**)^a

atom	x	y	z	B(A ²)
Nd	0.173 49 (4)	0.220 75 (4)	-0.117 81 (2)	1.807 (7)
Cl(1)	0.250	0.307 0 (3)	-0.250	2.21 (6)
Cl(2)	0.112 8 (2)	0.023 9 (2)	-0.176 1 (1)	2.26 (4)
Si	0.187 6 (2)	0.366 7 (2)	0.045 5 (1)	2.44 (5)
O(1)	0.145 6 (6)	-0.171 2 (6)	-0.301 5 (4)	4.0 (2)
C(1)	0.246 4 (9)	0.504 6 (8)	0.058 1 (5)	3.1 (2)
C(2)	0.140 3 (9)	0.335 (1)	0.142 8 (5)	4.2 (3)
C(3)	0.068 0 (7)	0.358 5 (7)	-0.032 0 (4)	2.1 (2)
C(4)	-0.012 3 (7)	0.271 2 (8)	-0.044 9 (5)	2.3 (2)
C(5)	-0.058 6 (7)	0.273 8 (7)	-0.121 0 (5)	2.2 (2)
C(6)	-0.010 7 (7)	0.360 0 (7)	-0.157 4 (5)	2.0 (2)
C(7)	0.069 5 (7)	0.411 0 (7)	-0.104 1 (5)	2.1 (2)
C(8)	0.292 1 (8)	0.265 2 (7)	0.012 1 (5)	2.3 (2)
C(9)	0.275 7 (7)	0.152 7 (7)	0.015 9 (5)	2.3 (2)
C(10)	0.345 6 (8)	0.102 2 (7)	-0.035 6 (5)	2.4 (2)
C(11)	0.404 1 (7)	0.182 6 (7)	-0.072 2 (5)	2.0 (2)
C(12)	0.373 0 (7)	0.282 0 (7)	-0.043 6 (5)	2.2 (2)
C(13)	-0.055 0 (9)	0.195 8 (9)	0.012 1 (5)	3.6 (2)
C(14)	-0.152 5 (8)	0.202 7 (9)	-0.155 7 (6)	3.6 (2)
C(15)	-0.046 6 (9)	0.398 3 (8)	-0.237 2 (5)	3.0 (2)
C(16)	0.136 4 (8)	0.511 2 (7)	-0.121 0 (5)	2.7 (2)
C(17)	0.209 9 (9)	0.091 1 (9)	0.072 4 (6)	4.0 (2)
C(18)	0.358 4 (9)	-0.015 2 (8)	-0.045 3 (6)	3.4 (2)
C(19)	0.492 3 (8)	0.165 3 (9)	-0.129 2 (5)	3.2 (2)
C(20)	0.427 3 (8)	0.386 6 (7)	-0.066 0 (5)	2.3 (2)
C(21)	-0.002 (1)	-0.294 0 (9)	-0.324 1 (7)	4.6 (3)
C(22)	0.189 (1)	-0.254 4 (9)	-0.348 2 (7)	4.8 (3)
C(23)	0.021 (1)	-0.184 (1)	-0.298 5 (8)	5.9 (3)
C(24)	0.087 (1)	-0.311 (1)	-0.379 6 (9)	7.4 (4)
Li	0.250	-0.068 (2)	-0.250	4.1 (6)

^a Anisotropically refined atoms are given in the form of the isotropic equivalent thermal parameter defined as $4/3[(a^2)B(1,1) + (b^2)B(2,2) + (c^2)B(3,3) + ab(\cos \gamma)B(1,2) + ac(\cos \beta)B(1,3) + bc(\cos \alpha)B(2,3)]$.

ceeding from $\text{Cp}'_2\text{ThX}_2$ complexes to $\text{Me}_2\text{SiCp}'_2\text{ThX}_2$ analogues, where the contraction is from 135 – 138° to 118.4° ($X = \text{CH}_2\text{Si}(\text{CH}_3)_3$).^{6,16} Also similar to the thorium systems, the Nd–C(ring) distances exhibit significant dispersion, with the longest distances being to the carbon atoms furthest from the silicon atom, i.e., Nd–C5 = 2.784 (7) Å, Nd–C6 = 2.815 (7) Å, Nd–C10 = 2.809 (7) Å, and Nd–C11 = 2.784 (7) Å. The shortest distances are Nd–C3 = 2.676 (7) Å and Nd–C8 = 2.647 (7) Å. In $\text{Cp}'_2\text{NdCH}(\text{TMS})_2$, the average Nd–C(ring) distance is 2.76 (1, 3, 8, 20)¹⁷ Å, while in $[(\text{CH}_3)_3\text{Si}]_2\text{C}_5\text{H}_3\text{NdCl}_2^+\text{As}(\text{C}_6\text{H}_5)_4^+$ (**8**)¹⁸ it is 2.78 Å. Interestingly, and in marked contrast to $\text{Me}_2\text{SiCp}'_2\text{Th}[\text{CH}_2\text{Si}(\text{CH}_3)_3]_2$,⁶ the present C(ring)–C(ring) distances do not evidence a marked dispersion; i.e., the shortest is C5–C6 = 1.402 (10) Å and the longest, C3–C4 = 1.449 (10) Å. In contrast, the C–C distances in the thorium complexes vary from 1.21 (3) to 1.56 (3) Å. The average C(ring)–CH₃ distance in **4** of 1.516 (10) Å is unexceptional.¹⁶ The present C3–Si–C8 angle of $101.0 (3)^\circ$ compares favorably with an angle of $100.1 (7)^\circ$ in $\text{Me}_2\text{SiCp}'_2\text{Th}[\text{CH}_2\text{Si}(\text{CH}_3)_3]_2$,⁶ also indicating that Si is displaced from each C5 ring mean plane—0.549 (3) Å for C3–C7; 0.535 (2) Å for C8–C12.

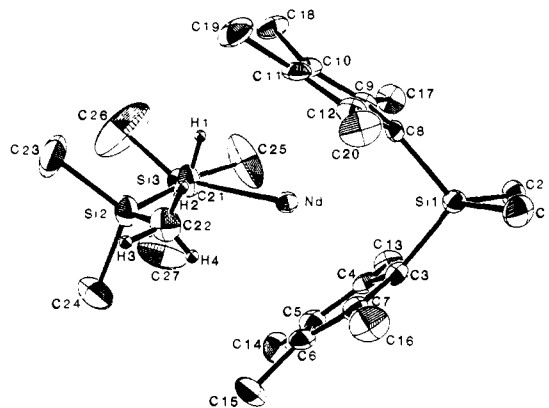
The NdCl₂ coordination in **4** is similar to that in other $\text{Cp}'_2\text{MX}_2$ ^{-14,15} complexes. Thus, the present Cl1–Nd–Cl2 angle of $97.1 (1)^\circ$ can be compared to Cl–M–Cl angles of $85.95 (2)^\circ$ in $\text{Cp}'_2\text{YbCl}_2\text{-Li}(\text{ether})_2^+$ (**9**),¹⁴ $87.14 (3)^\circ$ in $[(\text{C}_6\text{H}_5)_2(\text{CH}_3)_2\text{SiC}_5\text{H}_4]_2\text{YbCl}_2\text{-Li}(\text{ether})_2^+$ (**10**),¹⁴ $73.36 (3)^\circ$ in $\text{Cp}'_2\text{Yb}(\mu\text{-Cl})_2\text{AlCl}_2$ (**11**),¹⁴ and $99.3 (1)^\circ$ in (**8**).¹⁸ These com-

Table IV. Bond Lengths (Å) and Angles (deg) in Coordination Groups of $(\text{Me}_2\text{SiCp}'_2\text{Cl})_2\text{NdCl-Li}(\text{THF})_2^+$ (**4**)

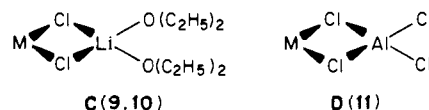
Bond Lengths			
Nd–Cl1	2.802 (1)	C4–C13	1.503 (10)
Nd–Cl2	2.754 (2)	C4–C5	1.414 (9)
Nd–C3	2.676 (7)	C5–C6	1.402 (10)
Nd–C4	2.695 (7)	C5–C14	1.505 (10)
Nd–C5	2.784 (7)	C6–C7	1.426 (9)
Nd–C6	2.815 (7)	C6–C15	1.522 (10)
Nd–C7	2.705 (7)	C7–C16	1.526 (10)
Nd–C8	2.647 (7)	C8–C9	1.431 (10)
Nd–C9	2.704 (7)	C8–C12	1.439 (10)
Nd–C10	2.809 (7)	C9–C10	1.425 (11)
Nd–C11	2.784 (7)	C9–C17	1.527 (10)
Nd–C12	2.688 (7)	C10–C11	1.410 (10)
Si–C1	1.872 (8)	C10–C18	1.497 (11)
Si–C2	1.901 (9)	C11–C12'	1.410 (10)
Si–C3	1.878 (7)	C11–C19	1.520 (10)
Si–C8	1.897 (8)	C12–C20	1.529 (10)
Li–C12	2.445 (11)	C21–C22	1.461 (16)
O–C21	1.454 (10)	C22–C23	1.503 (16)
O–C24	1.467 (11)	C23–C24	1.472 (13)
Li–O	1.955 (17)	O–C18	3.352 (11)
C3–C4	1.449 (10)	C18–C18' ^a	3.517 (17)
C3–C7	1.442 (9)		

Bond Angles			
Cl1–Nd–Cl2	97.1 (1)	C4–C3–C7	105.3 (6)
C3–Nd–C8	66.3 (2)	C3–C4–C5	108.8 (6)
C6–Nd–C10	163.1 (2)	C4–C5–C6	108.9 (6)
C4–Nd–C9	88.0 (2)	C5–C6–C7	107.9 (6)
C5–Nd–C10	142.0 (2)	C6–C7–C3	109.0 (6)
C6–Nd–C11	151.4 (2)	Si–C8–C9	124.1 (6)
C7–Nd–C12	94.5 (2)	Si–C8–C12	126.3 (6)
Nd–C12–Li	117.9 (4)	C12–C8–C9	106.0 (7)
Nd–C11–Nd	134.4	C8–C9–C10	108.9 (6)
C1–Si–C2	102.8 (4)	C9–C10–C11	107.6 (7)
C1–Si–C3	112.4 (4)	C10–C11–C12	108.7 (6)
C1–Si–C8	115.0 (4)	C11–C12–C8	108.7 (7)
C2–Si–C3	113.5 (4)	O–C21–C22	104.5 (8)
C2–Si–C8	112.7 (4)	C21–C22–C23	102.5 (9)
C3–Si–C8	101.0 (3)	C22–C23–C24	105.6 (9)
C21–O–C24	109.6 (7)	C23–C24–O	104.6 (9)
C21–O–Li	120.8 (6)	C12–Li–O	98.9 (2)
C24–O–Li	129.5 (6)	C12–Li–C12'	123.7
Si–C3–C4	125.9 (5)	O–Li–O	96.5
Si–C3–C7	124.7 (5)	Cg–Nd–Cg ^b	121.3

^a Prime refers to symmetry equivalent carbon atom in the other half of the dimer. ^b Cg = ring centroid.

**Figure 5.** Another ORTEP view of the molecular structure of $\text{Me}_2\text{SiCp}'_2\text{NdCH}(\text{TMS})_2$ (**5**). All non-hydrogen atoms are represented by thermal ellipsoids drawn to encompass 50% of the electron density.

plexes have bridging ligation as shown in **C** and **D**. The difference



between Nd–Cl1 = 2.802 (1) Å and Nd–Cl2 = 2.754 (2) Å distances presumably reflects the differing electronic demands

(16) (a) Bruno, J. W.; Marks, T. J.; Day, V. W. *J. Organomet. Chem.* **1983**, *250*, 237–246. (b) Fagan, P. J.; Manriquez, J. M.; Marks, T. J.; Vollmar, S. H.; Day, C. S.; Day, V. W. *J. Am. Chem. Soc.* **1981**, *103*, 2206–2220. (c) Fagan, P. J.; Manriquez, J. M.; Marks, T. J.; Day, V. W.; Vollmer, S. H.; Day, C. S. *J. Am. Chem. Soc.* **1980**, *102*, 5393–5396.

(17) The first number in parentheses following an averaged value of a bond length or angle is the root-mean-square estimated standard deviation of an individual datum. The second and third numbers, when given, are the average and maximum deviations from the averaged value, respectively. The fourth number represents the number of individual measurements which are included in the average value.

(18) Lappert, M. F.; Singh, A.; Atwood, J. L.; Hunter, W. E.; Zhang, H.-M. *J. Chem. Soc., Chem. Commun.* **1983**, 69–70.

Table V. Positional Parameters and Their Estimated Standard Deviations for $\text{Me}_2\text{SiCp}'_2\text{NdCH}(\text{TMS})_2$ (**5**)^a

atom	x	y	z	B(A2)
Nd	0.06627 (4)	0.03184 (3)	0.27859 (2)	1.671 (8)
Si(1)	0.1666 (2)	-0.0887 (2)	0.4286 (1)	1.87 (5)
Si(2)	0.0132 (3)	0.1709 (2)	0.1500 (1)	2.72 (6)
Si(3)	-0.2410 (3)	0.0424 (2)	0.1053 (1)	2.60 (6)
C(1)	-0.067 (1)	0.0676 (6)	0.1555 (5)	2.7 (2)
C(2)	0.1753 (9)	0.1792 (6)	0.2267 (5)	2.8 (2)
C(3)	-0.090 (1)	0.2673 (7)	0.1598 (7)	5.0 (3)
C(4)	0.076 (1)	0.1862 (8)	0.0695 (6)	5.3 (3)
C(5)	-0.296 (1)	-0.0621 (8)	0.1341 (9)	7.6 (4)
C(6)	-0.369 (1)	0.1200 (9)	0.1188 (9)	7.1 (4)
C(7)	-0.257 (2)	0.032 (1)	0.0085 (7)	10.4 (6)
C(8)	0.073 (1)	-0.1789 (6)	0.4581 (5)	2.7 (2)
C(9)	0.3300 (9)	-0.0816 (7)	0.5023 (5)	3.0 (2)
C(10)	0.2013 (8)	-0.1047 (5)	0.3406 (4)	1.5 (2)
C(11)	0.2998 (8)	-0.0588 (5)	0.3136 (5)	2.0 (2)
C(12)	0.2648 (8)	-0.0650 (6)	0.2392 (5)	2.2 (2)
C(13)	0.1446 (8)	-0.1159 (6)	0.2164 (5)	2.1 (2)
C(14)	0.1074 (8)	-0.1400 (5)	0.2780 (4)	1.8 (2)
C(15)	0.4211 (9)	-0.0105 (7)	0.3564 (5)	3.1 (2)
C(16)	0.3465 (9)	-0.0305 (7)	0.1901 (5)	3.4 (2)
C(17)	0.0861 (9)	-0.1484 (6)	0.1442 (5)	2.8 (2)
C(18)	-0.0061 (9)	-0.2042 (6)	0.2749 (5)	2.7 (2)
C(19)	0.0679 (8)	0.0139 (5)	0.4135 (4)	1.8 (2)
C(20)	0.1221 (9)	0.0988 (6)	0.4126 (4)	2.1 (2)
C(21)	0.0160 (9)	0.1539 (6)	0.3746 (5)	2.7 (2)
C(22)	-0.1049 (8)	0.1040 (6)	0.3520 (5)	2.4 (2)
C(23)	-0.0747 (8)	0.0200 (6)	0.3746 (4)	2.2 (2)
C(24)	0.259 (1)	0.1311 (6)	0.4516 (5)	3.3 (2)
C(25)	0.027 (1)	0.2504 (6)	0.3701 (6)	4.0 (3)
C(26)	-0.242 (1)	0.1420 (7)	0.3184 (5)	3.7 (2)
C(27)	-0.1808 (9)	-0.0509 (6)	0.3634 (5)	2.6 (2)
H(1)	0.0000	0.0214	0.1484	4*
H(2)	0.1933	0.2304	0.2148	4*
H(3)	0.1660	0.1875	0.2656	4*
H(4)	0.2500	0.1445	0.2324	4*

^aStarred atoms were refined isotropically. Anisotropically refined atoms are given in the form of the isotropic equivalent thermal parameter defined as $\frac{1}{3}[(a^2)B(1,1) + (b^2)B(2,2) + (c^2)B(3,3) + ab(\cos \gamma)B(1,2) + ac(\cos \beta)B(1,3) + bc(\cos \alpha)B(2,3)]$.

of Nd^{3+} and Li^+ in bridge formation. These Nd-Cl distances can be compared to nonbridging distances of 2.669 (3) and 2.667 (3) Å in **8**, (after a $\text{Yb}^{3+} \rightarrow \text{Nd}^{3+}$ ionic radius correction¹⁹) 2.720 (1) and 2.718 (1) Å in **9**, and 2.717 (1) Å in **10**. The Li-Cl distance of 2.445 (11) Å and Li-O distance of 1.955 (17) Å in **4** compare favorably with Li-Cl = 2.390 (6) and 2.412 (6) Å, Li-O = 1.924 (7) and 1.935 (7) Å in **9**, and Li-Cl = 2.390 (4) and Li-O = 1.957 (4) Å in **10**.

Molecular Structure of $\text{Me}_2\text{SiCp}'_2\text{NdCH}[\text{Si}(\text{CH}_3)_3]_2$ (5**).** Perspective views of compound **5** along with the atom labeling scheme are given in Figures 4 and 5. Final atomic coordinates and anisotropic thermal parameters are compiled in Tables V and VI,⁸ respectively. Important bond lengths and angles along with estimated standard deviations are presented in Table VII.

The $\text{Me}_2\text{SiCp}'_2$ ligation in **5** is rather similar to that in $(\text{Me}_2\text{SiCp}'_2\text{NdCl})_2\text{Cl-Li}(\text{THF})_2^+$ (**4**) while the $\text{CH}(\text{TMS})_2$ coordination (vide infra) is similar to, but more precisely defined than, that in the disordered structure of $\text{Cp}'_2\text{NdCH}(\text{TMS})_2$ (**12**).² Thus, the (ring centroid)-Nd-(ring centroid) angle in **5** is 121.6° and the C3-Si1-C8 angle, 101.2 (3)°. The C₅ rings are coplanar to within 0.006 (9) Å, while the methyl groups are displaced 0.02-0.19 (1) Å from the C₅ mean planes in a direction away from the Nd ion. As in **4**, the longest Nd-C(ring) distances are for the carbon atoms furthest from the Me_2Si bridge. As in **4**, the alternation in framework C-C distances about the C₅ rings is rather small. Detailed comparison of Tables IV and VII shows that the Nd-C(ring) and intra- $\text{Me}_2\text{SiCp}'_2$ metrical parameters in **4** and **5** are in close agreement.

The $\text{CH}(\text{TMS})_2$ ligation in **5** involves a highly unsymmetrical

Table VII. Bond Lengths (Å) and Angles (deg) in Coordination Groups of $\text{Me}_2\text{SiCp}'_2\text{NdCH}(\text{TMS})_2$ (**5**)

Bond Lengths			
Nd-C21	2.506 (7)	Si3-C25	1.865 (10)
Nd-C22	2.862 (8)	Si3-C26	1.856 (10)
Nd-C3	2.655 (6)	Si3-C27	1.875 (12)
Nd-C4	2.705 (7)	C3-C4	1.448 (9)
Nd-C5	2.803 (7)	C3-C7	1.454 (9)
Nd-C6	2.825 (7)	C4-C13	1.503 (10)
Nd-C7	2.716 (7)	C4-C5	1.416 (10)
Nd-C8	2.664 (7)	C5-C6	1.433 (10)
Nd-C9	2.752 (7)	C5-C14	1.535 (10)
Nd-C10	2.825 (7)	C6-C7	1.415 (10)
Nd-C11	2.788 (7)	C6-C15	1.478 (10)
Nd-C12	2.671 (7)	C7-C16	1.523 (10)
Si1-C1	1.882 (8)	C8-C9	1.438 (10)
Si1-C2	1.904 (8)	C8-C12	1.460 (10)
Si1-C3	1.874 (7)	C9-C10	1.430 (10)
Si1-C8	1.875 (7)	C9-C17	1.497 (10)
Si2-C21	1.827 (8)	C10-C11	1.430 (11)
Si2-C22	1.928 (8)	C10-C18	1.515 (11)
Si2-C23	1.878 (10)	C11-C12	1.394 (10)
Si2-C24	1.874 (9)	C11-C19	1.508 (10)
Si3-C21	1.834 (8)	C12-C20	1.525 (10)
Bond Angles			
C3-Nd-C8	66.0 (2)	Si1-C3-C4	126.4 (5)
C6-Nd-C10	164.4 (2)	Si1-C3-C7	126.0 (5)
C4-Nd-C9	90.6 (2)	C4-C3-C5	104.2 (6)
C5-Nd-C10	145.4 (2)	C3-C4-C5	109.6 (6)
C6-Nd-C11	147.6 (2)	C4-C5-C6	108.8 (6)
C7-Nd-C12	92.7 (2)	C5-C6-C7	106.6 (6)
C1-Si1-C2	103.1 (4)	C6-C7-C3	110.9 (6)
C1-Si1-C3	115.0 (3)	Si1-C8-C9	126.6 (5)
C1-Si1-C8	113.0 (3)	Si1-C8-C12	124.0 (5)
C2-Si1-C3	111.6 (3)	C12-C8-C9	105.6 (6)
C2-Si1-C8	113.4 (3)	C8-C9-C10	108.6 (6)
C3-Si1-C8	101.2 (3)	C9-C10-C11	108.0 (7)
C21-Si2-C22	108.7 (3)	C10-C11-C12	108.2 (6)
C21-Si2-C23	115.3 (4)	C11-C12-C8	109.5 (6)
C21-Si2-C24	115.0 (4)	Nd-C21-Si2	96.7 (3)
C21-Si3-C25	110.8 (4)	Nd-C21-Si3	132.4 (4)
C21-Si3-C26	113.9 (4)	Si2-C21-Si3	123.0 (4)
C21-Si3-C27	112.1 (5)	Cg-Nd-Cg ^a	121.6

^aCg = ring centroid.

Nd-hydrocarbyl interaction, which is particularly evident in Figure 4. Thus, the Nd-C21-Si3 angle is 132.4 (4)° while the Nd-C21-Si2 angle is 96.7 (3)° (the corresponding angles in **12**² are 140.15 (43)° and 98.44 (31)°). Skewing of the Nd-CH(TMS)₂ interaction is also evident in the Si1-Nd-C21 angle of 156.6 (2)°. Atoms Nd, C21, Si2, and Si3 are coplanar to within 0.04 (1) Å (vs. 0.02 (1) Å in **12**). At least part of the valence angle expansion about C21 must reflect the steric bulk of the TMS groups, since similar expansions have been observed in $\text{H}_2\text{C}[\text{Si}(\text{CH}_3)_3]_2$, 123.2 (9)°, and $\text{HC}[\text{Si}(\text{CH}_3)_3]_3$, 116.3 (4)°.²⁰

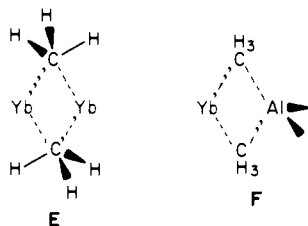
As in **12**,² the primary Nd-hydrocarbyl interaction in **5** (Nd-C21 = 2.506 (7) Å) is supplemented by a significant secondary interaction to a single methyl group: Nd-C22 = 2.862 (8) Å (these distances are 2.517 (7) and 2.895 (7) Å in **12**). The average of all Si-CH₃ distances in **5** other than Si2-C22 is 1.870 (10, 7, 17, 5) Å, in good agreement with distances in other trimethylsilyl compounds (usually about 1.873 Å).²⁰ The distances C21-Si2 = 1.827 (8) Å and C21-Si3 = 1.834 (8) Å are slightly shorter than the corresponding lengths in molecules such as $\text{H}_2\text{C}[\text{Si}(\text{C}-\text{H}_3)_3]_2$ (1.889 (4) Å). The mutually "eclipsed" conformation of the two $\text{Si}(\text{CH}_3)_3$ groups in **5** is identical with that in $\text{H}_2\text{C}[\text{Si}(\text{CH}_3)_3]_2$.²⁰ Interestingly, Si2-C22 is 1.928 (8) Å, a value which appears to be significantly longer than the aforementioned average of the other Si-CH₃ distances. The Nd-CH(TMS)₂ orientations in **5** and **12** are thus rather similar, despite the "pulled-back" permethylcyclopentadienyl ligands in **5**. It seems

(20) (a) Eaborn, C.; Hitchcock, P. B.; Lickies, P. D. *J. Organomet. Chem.* **1984**, *269*, 225-238 and references therein. (b) Fieldberg, T.; Seip, R.; Lappert, M. F.; Thorne, A. J. *J. Mol. Struct.* **1983**, *99*, 295-302 and references therein. (c) Beagley, B.; Pritchard, R. G. *J. Mol. Struct.* **1982**, *84*, 129-139.

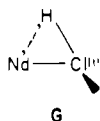
(19) (a) Representative eight-coordinate effective ionic radii^{32b}: La^{3+} (1.160 Å), Nd^{3+} (1.109 Å), Sm^{3+} (1.079 Å), Yb^{3+} (0.985 Å), and Lu^{3+} (0.977 Å). (b) Shannon, R. D. *Acta Crystallogr., Sect. A* **1976**, *A32*, 751-767.

unlikely, then, that the close Nd–C22 contact and the elongated Si2–C22 bond are the result of nonbonded repulsive interactions rather than attractive bonding interactions.

Figures 4 and 5 show the hydrogen atoms bound to carbon atoms C21 and C22. The hydrogen atoms in **5** could be readily located in the difference Fourier calculation, and although the associated metrical parameters must be viewed with appropriate precautions²¹ and are clearly no substitute for neutron diffraction data, significant qualitative remarks can be made. First, the disposition of hydrogen atoms H2, H3, and H4 does not minimize any particular Nd–H distance as in many "agostic" C–H...M structural motifs.²² Rather, the hydrogen atom disposition (as well as the Si2–C22 lengthening) is more reminiscent of three-center, two-electron bridging alkyl bonding, the extreme organolanthanide examples of which are found in [Cp₂M(μ-CH₃)₂]₂ (**E**) and Cp₂M(μ-CH₃)₂Al(CH₃)₂ (**F**) compounds.²³ As noted



for **12**,² the close Nd–C contact, the lengthening of Si2–C22, and the syn-periplanar conformation are structurally suggestive of a β-methyl²⁴ elimination scenario which is aborted due to the unacceptable high energy content²⁵ of the resulting Si=C moiety. Also noteworthy in **5** is the curious position of the hydrogen atom H1—bent toward the Nd ion with ∠Nd–C21–H1 ~ 76°. This arrangement results in a Nd–H1 distance of ca. 2.5 Å (assuming C21–H1 = 1.09 Å), which can be compared with neutron-diffraction-derived Th–H terminal and bridge distances of 2.03 (1) and 2.29 (3) Å, respectively, in [Cp₂Th(μ-H)H]₂.²⁵ Correcting for differences in eight-coordinate radii,¹⁹ Nd–H distances of ca. 2.09 and 2.37 Å are estimated for terminal and fully bridging configurations. Although part of this "agostic" or semibridging CHNd interaction no doubt reflects the near planarity of the Nd, C21, Si2, and Si3 fragment, which in turn must reflect the bulkiness of the C21 substituents,²⁰ it also appears likely that part of the interaction reflects the high electrophilicity and electron deficiency at the metal center (e.g., **G**). Such



interactions occur in early transition-metal alkylidene and alkylidyne systems.^{21b,27,28} More relevant to f-element complexes, a similar interaction is observed in neutron diffraction studies of

(21) (a) Teller, R. G.; Bau, R. *Struct. Bond. (Berlin)* **1981**, *44*, 2–82. (b) Schultz, A. J.; Brown, R. K.; Williams, J. M.; Schrock, R. R. *J. Am. Chem. Soc.* **1981**, *103*, 169–176. (c) Marks, T. J.; Kolb, J. R. *Chem. Rev.* **1977**, *77*, 263–293.

(22) Brookhart, M.; Green, M. L. H. *J. Organomet. Chem.* **1983**, *250*, 395–408 and references therein.

(23) (a) Holton, J.; Lappert, M. F.; Ballard, D. G. H.; Pearce, R.; Atwood, J. L.; Hunter, W. E. *J. Chem. Soc., Dalton Trans.* **1979**, 54–61. (b) Holton, J.; Lappert, M. F.; Ballard, D. G. H.; Pearce, R.; Atwood, J. L.; Hunter, W. E. *J. Chem. Soc., Dalton Trans.* **1979**, 45–54.

(24) Watson, P. L.; Roe, D. C. *J. Am. Chem. Soc.* **1982**, *104*, 6471–6473.

(25) Brook, A. G.; Nyburg, S. C.; Abdesaken, F.; Gutekunst, B.; Gutekunst, G.; Kalury, R. K. M. R.; Poon, Y. C.; Chang, Y.-M.; Wong-Ng, W. *J. Am. Chem. Soc.* **1982**, *104*, 5667–5672 and references therein.

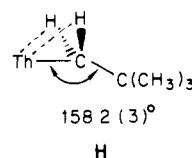
(26) Broach, R. W.; Schultz, A. J.; Williams, J. M.; Brown, G. M.; Manriquez, J. M.; Fagan, P. J.; Marks, T. J. *Science (Washington, D.C.)* **1979**, *203*, 172–174.

(27) (a) Schrock, R. R. In "Reactions of Coordinated Ligands"; Brateman, P., Ed.; Plenum Press: New York, 1983. (b) Churchill, M. R.; Wasserman, H. J. *Inorg. Chem.* **1983**, *22*, 1574–1578 and references therein.

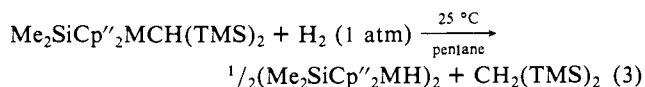
(28) Goddard, R. J.; Hoffman, R.; Jemmis, E. D. *J. Am. Chem. Soc.* **1980**, *102*, 7667–7676.

(29) Bruno, J. W.; Smith, G. M.; Marks, T. J.; Fair, K.; Schultz, A. J.; Williams, J. M. *J. Am. Chem. Soc.*, in press.

Cp₂Th[CH₂C(CH₃)₂]₂.²⁹ Here, relatively close Th–H interactions (∠Th–C–H = 84.4 (5)° and 87.1 (5)° and Th–H = 2.597 (9) and 2.648 (9) Å, respectively) are associated with the methylene H atoms of one highly distorted neopentyl ligand (**H**).



Synthesis. Hydrides. Compounds **5**, **6**, and **7** react rapidly with hydrogen to yield the corresponding hydrides (eq 3). Qualitatively, the hydrogenolysis of a given Me₂SiCp₂MCH(TMS)₂ complex is more rapid under the same conditions than is hydrogenolysis of the analogous Cp₂MCH(TMS)₂ complex. Hydrides **13–15**



13, M = Nd **13d**, H = D

14, M = Sm **14d**, H = D

15, M = Lu **15d**, H = D

are less soluble than the (Cp₂MH)₂ analogues² and can be isolated from reaction 3 in essentially quantitative yield after filtration and washing. ¹H NMR data are given in the Experimental Section. Exchange of metal-bound hydride with toluene-*d*₈ deuterons is qualitatively more rapid than for the (Cp₂MH)₂ analogues,² and the hydride signals for the Me₂SiCp₂M Sm and Lu hydrides could only be observed under an atmosphere of H₂. As in the case of the Cp₂MX systems, progression from X = CH(TMS)₂ to X = H renders the permethylcyclopentadienyl ligands magnetically equivalent. Complex **13** is dimeric in benzene solution by cryoscopy.

Infrared spectral data for **13–15**, **13d**, and **15d** are collected in the Experimental Section. Unlike the (Cp₂MH)₂/(Cp₂MD)₂ complexes, where the infrared spectra of the M = Lu derivatives differ significantly from those of other M derivatives, the spectra of the present hydrides are essentially independent of M, suggesting very similar molecular structures. Because of interfering Me₂SiCp₂-centered vibrational modes, assignments of M–H/M–D transitions cannot be as detailed as in the (Cp₂MH)₂ series. Nevertheless, a broad band at ca. 1120 cm⁻¹ is again observed, which shifts to ca. 820 cm⁻¹ in the deuterated derivatives (ν_{M–H}/ν_{M–D} ≈ 1.37). Taken together with mass spectral and cryoscopic molecular weight data, these results suggest a dimeric M(μ-H)₂M structure (I). This formulation is consistent with the solubility

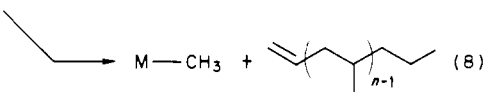
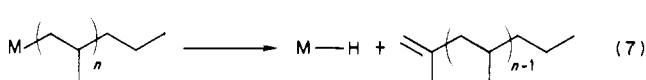
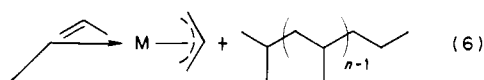
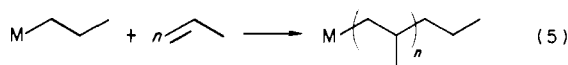
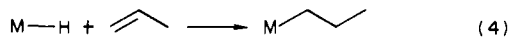


properties and olefin hydrogenation kinetics, which show that rate laws for bulky olefins are half-order in metal hydride.³ That both (Cp₂ThH)₂²⁶ and (Me₂SiCp₂ThH)₂^{6b} has been shown to be dimeric in diffraction studies also supports this proposal.

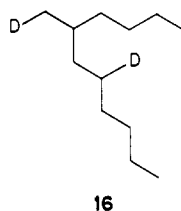
Reaction Chemistry with Olefins. Comparison to (Cp₂MH)₂ Complexes. It was also of interest to determine whether the altered permethylcyclopentadienyl disposition in the Me₂SiCp₂ complexes significantly modified reactivity with respect to olefin insertion. Thus, to the extent that it was possible, reactions were carried out by using procedures identical with those for analogous (Cp₂MH)₂ compounds.² One complication was the significantly lower solubility of the (Me₂SiCp₂MH)₂ complexes. Thus, for ethylene polymerization experiments, catalyst concentrations were at such a dilute level that poisoning by trace contaminants became possible. Nevertheless, for (Me₂SiCp₂NdH)₂ at 25 °C, 1 atm of ethylene pressure, an N₁ value of 1.6 s⁻¹ was measured for polymerization.

Catalyst solubilities were less of a problem for the slower propylene and 1-hexene reactions since additional quantities of the hydrides dissolved upon olefin addition. In situ ¹H NMR

studies revealed rapid consumption of the hydrides and the formation of multiple products. No interpretation was attempted since other data (vide infra) indicate that olefin insertion is more facile for the $\text{Me}_2\text{SiCp}''_2$ complexes. Reaction of $(\text{Me}_2\text{SiCp}''_2\text{LuH})_2$ with propylene was studied in cyclohexane at 25 °C (4.0-atm gauge pressure) and at 66 °C (6.5-atm gauge pressure). Yields of propylene oligomers were approximately 10 times those in the $(\text{Cp}'_2\text{LuH})_2$ -catalyzed reaction under the same conditions.² For the 66 °C reaction, GC/MS data revealed a complex product mixture with greater than 20 components having carbon contents at least as high as C_{21} . A reasonable mechanism for hydride-induced propylene oligomerization followed, inter alia, involve olefin insertion into the lanthanide-hydride bond (eq 4), followed, inter alia, by sequential olefin insertion into the resulting lanthanide-carbon bond (e.g., eq 5)^{2,14} and termination by olefin metalation (e.g., eq 6),² β -hydrogen elimination (eq 7),^{2,14} or β -methyl elimination (eq 8).^{14,24} As already noted,² slowly stirring



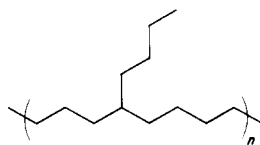
a $(\text{Cp}'_2\text{MH})_2$ complex in 1-hexene under a D_2 atmosphere yields the saturated 1-hexene dimerization product **16** with less than 1% of the total oligomer yield consisting of trimers, etc. When this



16

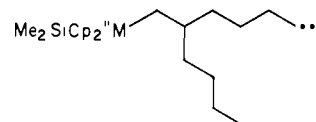
reaction was carried out with $(\text{Me}_2\text{SiCp}''_2\text{LuH})_2$ under identical conditions, the yield of **16** was ca. 8 times that with $(\text{Cp}'_2\text{LuH})_2$.² In addition, small quantities (given as a percentage of total oligomer yield) of the hexane oligomers $\text{C}_{18}\text{H}_{36}\text{D}_2$ (7.4%), $\text{C}_{24}\text{H}_{48}\text{D}_2$ (0.3%), $\text{C}_{30}\text{H}_{60}\text{D}_2$ (0.03%), and $\text{C}_{36}\text{H}_{72}\text{D}_2$ (0.01%) were detected by GC/MS. Additional 1-hexene insertions followed by deuterolysis of the Lu-C bond² explain the presence and isotopic substitution of these higher oligomers.

Stirring 70 mg of $(\text{Me}_2\text{SiCp}''_2\text{LuH})_2$ in 30 mL of 1-hexene under 1 atm of ethylene for 10 min yielded, after quenching and workup, 3.5 g of a rubbery ethylene/1-hexene copolymer. By ¹³C



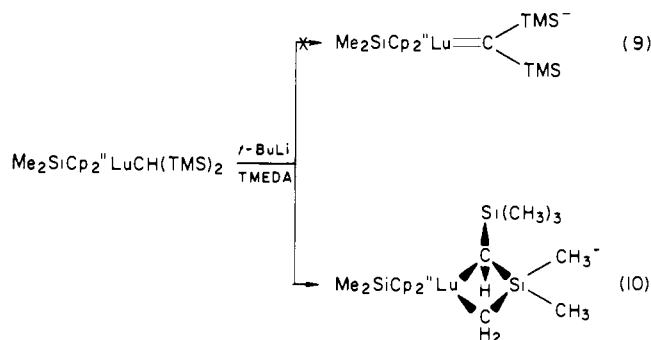
17

NMR, the ratio of ethylene/1-hexene in the polymer was determined to be ca. 3:1 (e.g., **17**). These results indicate, not surprisingly, that the rate of chain propagation is highly sensitive to the steric bulk that must be incorporated near the metal center. Thus, while configuration **18** cannot support rapid 1-hexene insertion, ethylene insertion is relatively facile.



18

Deprotonation of $\text{Me}_2\text{SiCp}''_2\text{LuCH}(\text{TMS})_2$. Attempted Alkylidene Formation. Efforts to abstract a proton from the α -carbon atom of **7** did not yield an alkylidene (eq 9). Rather, a Li-(TMEDA)₃⁺ salt was isolated (satisfactory elemental analysis) which was assigned a metallacyclobutane structure (eq 10) on the basis of NMR spectroscopy. (See Experimental Section for



data.) Thus, nonequivalent metallacyclic LuCH_2 (an AB pair) and SiMe_2 signals are observed along with SiMe_3 and LuCH singlets. Moreover, lowering of the $\text{Me}_2\text{SiCp}''_2$ symmetry from C_s is clearly evident. It thus appears that the γ -carbon atom deprotonation product is the most thermodynamically stable.

Conclusions

This work demonstrates that it is possible to generate a series of ring-connected lanthanide hydrocarbyl and hydride derivatives which parallel the previously described² $\text{Cp}'_2\text{MCH}(\text{TMS})_2$, $(\text{Cp}'_2\text{MH})_2$ series. While gross structural features and reaction pathways are similar for analogous $\text{Cp}'_2\text{M}$ and $\text{Me}_2\text{SiCp}''_2\text{M}$ derivatives, significant reactivity increases are observed in the latter series for sterically sensitive processes such as olefin insertion into the $\text{Cp}'_2\text{MR}/\text{Me}_2\text{SiCp}''_2\text{MR}$ metal-carbon σ bond. The degree to which such modifications can affect reaction rates in olefin hydrogenation catalysis is explored in the preceding paper in this issue.³

Acknowledgment. This research was supported by a grant from MolyCorp. and the National Science Foundation (CHE8306255 to T.J.M.). G. J. thanks the Fonds der Chemischen Industrien for fellowship support during his stay in the United States. We thank Dr. C. M. Fendrick for advice concerning the ligand synthesis.

Supplementary Material Available: Anisotropic thermal parameters for compounds **4** and **5** (Tables III and VI, respectively), and structure factor tables for **4** and **5** (78 pages). Ordering information is given on any current masthead page.